Airborne Reflector-Based Ground Penetrating Radar for Environmental and Archaeological Studies

ZAYED MOHAMMAD (Member, IEEE), AND **ANDREW M. CHRYSLER** (Member, IEEE)

Department of Electrical and Computer Engineering, Idaho State University, Pocatello, ID 83209, USA

CORRESPONDING AUTHOR: Z. MOHAMMAD (e-mail: zayedmohammad@isu.edu)

ABSTRACT In this work, a wideband airborne reflector-based ground penetrating radar (GPR) is designed and proposed. The proposed GPR consists of 15 discrete panels, each panel supported by a single multi-rotor unmanned aerial vehicle (UAV). A lightweight, wideband Vivaldi antenna was developed as the feed structure. The antenna operates within the frequency range of 100-500 MHz and has a bandwidth of 387 MHz. The proposed antenna will possess a penetration depth of 2 m. Different panel configurations are studied and it is found that 15 discrete panels each with a dimension of 30 cm by 4 m and separated by 30 cm acts as a reflector antenna with a high gain of 14.25 dBi.

INDEX TERMS Airborne, discrete parabolic reflector, ground penetrating radar, unmanned air vehicle, Vivaldi antenna.

I. INTRODUCTION

IN THE fields of engineering and geophysics, Ground-Penetrating Radar (GPR) has a wide range of different applications including geology, archaeology, mineral exploration, glaciology, civil engineering, and more [1]. In [2] the application of ground-penetrating radar (GPR) for the exploration and characterization of limestone deposits has been discussed. The study demonstrates that the 3-D visualization of GPR data enhances the understanding of limestone distribution and facilitates more accurate reserve estimations. The findings highlight the potential of GPR as a useful tool for limestone exploration and mining operations. The application of ground-penetrating radar (GPR) in archaeology has been explored in [3]. It highlights two main aspects: the ability of GPR to map significant areas of archaeological sites that would otherwise remain invisible using traditional excavation methods, and the advancements in data acquisition and processing techniques. In [4] the use of Ground Penetrating Radar (GPR) in civil engineering and its potential applications in monitoring the earth and construction materials has been discussed. It emphasizes that GPR can effectively be utilized for civil engineering purposes, as the most commonly used construction materials such as concrete, asphalt, soils, and rocks are mineral aggregates that can be examined using GPR. A helicopter-borne GPR for environmental

geology, and glaciology has been studied in [5]. The authors describe two types of radar systems: pulse radar and stepped-frequency radar (SFR). They explain that pulse radar systems have been used for measuring ice thickness, while SFR technology offers advantages such as reduced interference and high vertical resolution. The authors provide examples of survey data obtained using the pulse radar system, demonstrating its capability to measure bedrock reflections in thick Antarctic ice. They also present test results from the SFR system, conducted in different geological settings, including a military firing range and a glacier area in the Swiss Alps. However, to inspect and survey these rough, steep slopes, and hard-to-reach terrain, air-borne GPR plays a crucial role. By utilizing air-borne GPR, these challenging terrains will become more accessible. This technology will significantly enhance the survey process, making it more convenient and user-friendly.

Due to the wide range of GPR applications, various GPR antenna designs are commercially available, as well as utilized within the academic community for research purposes. GPR antenna type and size typically depend on the intended application. For instance, low frequency antennas that are larger in size are utilized when significant depth of penetration is crucial, while high frequency antennas that are smaller in size are employed when improved resolution and reduced
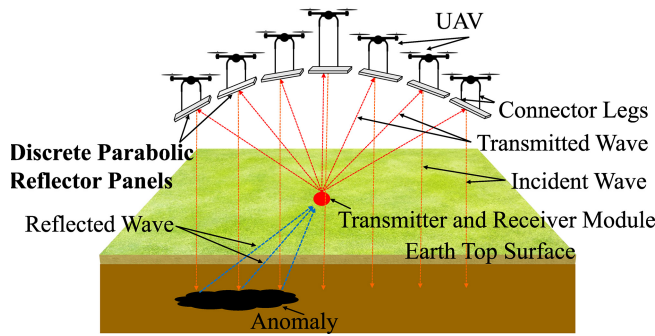
FIGURE 1. Illustration of the overall proposed concept, including the deployment of the discrete parabolic reflector supported by the UAV.

penetration are necessary [6]. Airborne GPR is a prominent electromagnetic technology applied to identify surface or shallow subsurface features and for large-scale studies of hard-to-reach areas [7], [8], [9]. However, the most important challenge for this airborne GPR system is the antenna design. Airborne GPRs require antennas that have a wide bandwidth and high gain to effectively transmit and receive signals from elevated altitudes [7]. In [7] an ultrawideband (UWB) antipodal Vivaldi antenna is considered as an airborne GPR with a maximum gain of 11.5 dBi. Both the transmitter and the receiver antenna were installed on a wooden frame and hovered using a rope. The setup was placed 1.5 m above the ground and targeted object was buried 150 mm beneath the ground. A dual-polarized Vivaldi antenna array consisting of 8×8 elements for airborne radar measurements of snow was proposed in [8]. The antenna was mounted on a fixed-wing aircraft flown at an altitude of 500 m. In [9] different types of UWB Vivaldi antennas and their performance were analyzed in the context of an airborne-based GPR system for landmine and IED detection. The antennas were arranged in Rx-Tx-Rx configuration and were installed on a multi-rotor unmanned aerial vehicle (UAV). The prototype was placed 1.5 m above the ground with a maximum penetration depth of 18 cm.

The aim of this work is to develop an airborne multi-rotor UAV based lightweight broadband GPR antenna, operating at a lower frequency band with high gain. Moreover, we propose a novel idea to increase the gain of the antenna by implementing parabolic reflector composed of discrete panels which could be supported by the UAV payload, depicted in Fig. 1. The proposed antenna will be portable, usable on rough and inaccessible terrain, and capable of hovering for extended periods over an area of interest.

Reflector antennas have applications such as satellite communications, radio astronomy, remote sensing, radar, weaponry, and medical applications [10]. Among reflector antennas, the parabolic reflector is one of the most desirable because of its improved overall radiation characteristics [11] and it is also recognized as more compatible antenna for radiometry because it has lower sidelobes and higher main beam efficiencies [12].
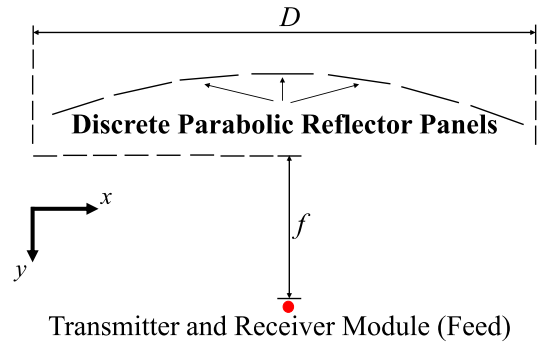

FIGURE 2. Geometric configuration of the discrete parabolic reflector and the feed in $y - x$ plane.
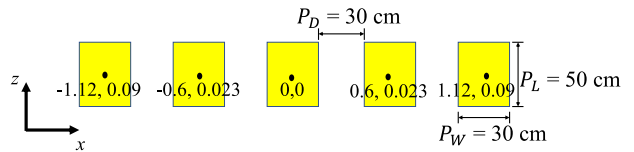

FIGURE 3. 2D view of the 5 discrete parabolic reflector panels out of a total of 15 in $x - z$ plane along the continuous parabola.

In Section II we describe the design methodology of both the discrete parabolic reflector and the feed antenna. Results and the outputs are analyzed and discussed in Section III. Finally, in Section IV we conclude and discuss the future works.

II. DESIGN METHODOLOGY
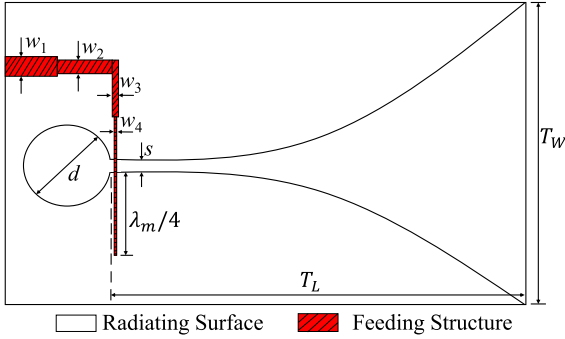### A. DESIGN PROCEDURE OF THE DISCRETE PARABOLIC REFLECTOR

The design procedure for the center-fed parabolic reflector is comprehensively explained in [13]. The parabolic reflector design is shown in Fig. 2. The fundamental parameters that guide the design are the focal length, f, and the diameter of the parabola, D, depicted in Fig. 2. Initially, a parabolic reflector with an f/D ratio of 0.4 was designed based on equation (1) and the value of the D was kept 10 m and f of 4 m.

$$x^2 + y^2 = 4f(f - z) \quad (1)$$

Afterward, in order to design a discrete parabolic reflector, 15 discrete rectangular metal panels were placed along the tangent of the continuous reflector. The distance between each of the rectangular sheets, P_D was kept $\lambda_0/10$, where λ_0 is the operating wavelength, here we considered 100 MHz as the minimum operating frequency. The panel reflectors are analogous to wire-grid reflectors, so the spacing between each of the rectangular panels was kept $\lambda_0/10$ according to wire-grid reflector spacing rule [11]. Initially, the length, P_L, and the width, P_W, of each of the metal panels were kept 50 cm and 30 cm respectively as shown in Fig. 3. The first metal panel was placed at (0, 0) coordinates of the continuous parabola in $x-z$ plane. To keep a distance of P_D between the two adjacent metal panels, the x coordinate of the next panel along the continuous parabolic axis was calculated then

TABLE 1. Parameters of the panels.

Panel Length P_L (cm)	50
Panel Width P_W (cm)	30
Panel Spacing P_D (cm)	30
Parabolic arc Diameter D (m)	10
Focal Length F (m)	4
Number of panels	15

TABLE 2. Parameters of the feed Vivaldi antenna.

Parameters	T_L	T_W	d	s
Value (m)	0.975	1	0.23	0.012
Parameters	w_1	w_2	w_3	w_4
Values (mm)	0.012	6	3.5	0.66

FIGURE 4. Design configuration of the proposed feed Vivaldi antenna.

equation (2) [16].

$$y = K_1 e^{Rx} + K_2 \tag{2}$$

In equation (2) R is the opening rate of the profile which was considered at 10.5, and K_1 and K_2 are determined by the coordinates of the starting and end point of the exponential curve using the equations (3) and (4), described below [16].

$$K_1 = \frac{y_2 - y_1}{e^{Rx_2} - e^{Rx_1}} \tag{3}$$

$$K_2 = \frac{y_1 e^{Rx_2} - y_2 e^{Rx_1}}{e^{Rx_2} - e^{Rx_1}} \tag{4}$$

According to [17], in order to radiate electromagnetic energy from the taper slots, the separation between the two flares needs to be greater than $\lambda_c/2$, where λ_c is the center frequency of the whole operating bandwidth. So, the starting and end point was chosen in such a way so that the taper length T_L and the taper width, T_W, is greater than $\lambda_c/2$.

The lower frequency limit is primarily determined by the antenna's width and the effective dielectric constant of the substrate, and can be determined using the equation (5) below [17]

$$f_0 = \frac{c}{2T_W \sqrt{\epsilon_{eff}}} \tag{5}$$

Here, f_0, is the minimum operating frequency and ϵ_{eff} is the effective dielectric constant of the substrate. The taper slot was terminated by a circular slot with a diameter, d, equivalent to one quarter-wavelength at the center frequency to further broaden the bandwidth. A microstrip to slotline transition feeding structure was designed to feed the antenna using a three-stage quarter-wave balun feeding. The feeding structure was designed using binomial multisection matching quarter-wave transformer. The initial feeding microstrip line was designed to have an input impedance of 50 Ω and the corresponding width, w_1, was kept at 6 mm. Then the three-stage multisection transformer was designed for improved impedance transition. The width of each of the multisection w_2, w_3, w_4 were set to 5.4 mm, 3.5 mm, and 0.66 mm corresponding to 55.5 Ω, 70 Ω, and 130.5 Ω, respectively. The length of each of the microstrip was kept $\lambda_m/4$, where λ_m is the microstrip guided wavelength. Moreover, to have a better impedance matching bandwidth the feeding microstrip line was also extended by a quarter-wavelength short circuit on the left side of the feeding line [18]. The optimized designed parameters are in Table 3.

by substituting the value of x in equation (1) we determined the corresponding z coordinate. A detailed 2D positioning of 5 panels out of 15, along the continuous parabola is also illustrated in Fig. 3. For designed panel size of 30 cm by 50 cm, spacing, and the diameter of 10 m of the parabolic arc, a total of 15 panels is the upper limit on a single parabolic arc. Moreover, it is anticipated that a 15 UAV system represents a reasonable number of drones to control simultaneously. The limits of this control system would be further explored in future works. Detailed panel parameters are tabulated in Table 1.

B. FEEDING TECHNIQUES

The feeding structure for the parabolic reflector depends on various factors, such as the designed frequency, desired directivity, gain, polarization and the application requirements. In this work we designed a Vivaldi antenna as a feeding structure. The Vivaldi antenna was considered because we required a light weight antenna with broadband impedance matching, unidirectional radiation, compact size, and high directivity as GPR system requires a broadband antenna with high gain [7]. Moreover, this airborne reflector based GPR requires a lightweight antenna to ensure maximum flight time and minimal payload.

The geometry of the proposed feed antenna is depicted in Fig. 4. The antenna was designed to have a minimum operating frequency of 100 MHz and a maximum operating frequency was considered 500 MHz. This frequency band was chosen according to FCC guidelines for GPR operation below 960 MHz [14], [15]. The substrate is FR4 with a dielectric constant, ϵ_r of 4.3, and loss tangent, tan δ, of 0.025. The FR4 substrate has a thickness of 3.2 mm. The exponentially tapered slots can be determined by using

III. RESULT ANALYSIS

The Vivaldi antenna was designed and simulated using CST Microwave Studio Suite. Fig. 5 shows the reflection

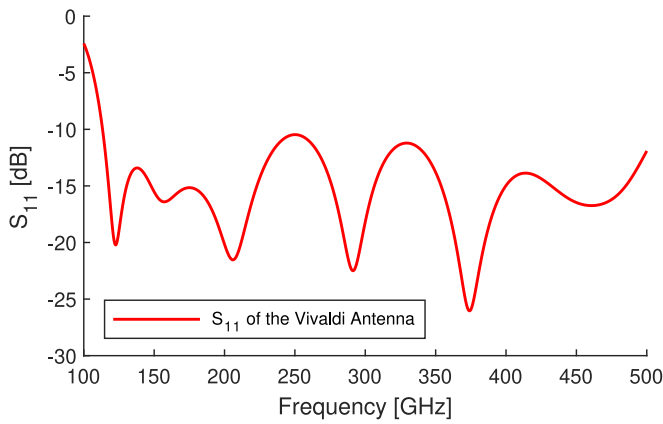**FIGURE 5.** S_{11} (< −10 dB) of the feed Vivaldi antenna. The operational frequency band is from 117 MHz to 500 MHz.
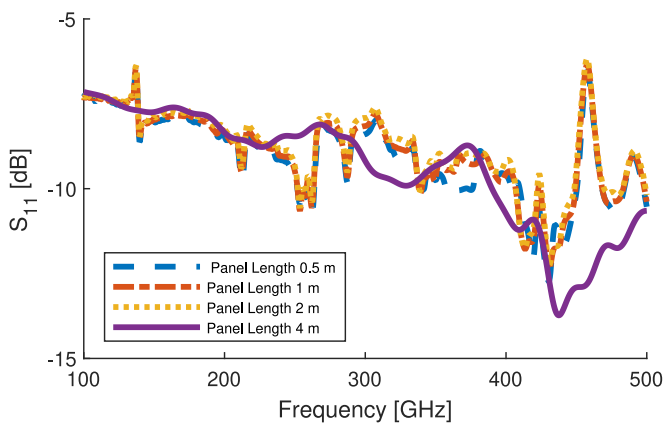

FIGURE 6. S_{11} (< −10 dB) of the feed Vivaldi antenna. The operational frequency band is from 117 MHz to 500 MHz.

FIGURE 7. IEEE gain comparison of the feed antenna without reflectors and with reflectors of different dimensions.

FIGURE 8. Far-field pattern for each of the reflector panels at 425 MHz (a) 50 cm panels (b) 1m panels (c) 2 m panels (d) 4 m panels.

coefficient of the designed Vivaldi antenna. The antenna operates within the whole operating band of 117 - 500 MHz and has a wide bandwidth of 387 MHz. The discrete reflector panels are deployed as a center feed parabolic reflector antenna to enhance the gain of the antenna. To determine panel sizing in simulations, a reflector panel dimension of 30 cm by 50 cm was initially considered. Then, panel dimensions gradually increased. To increase dimensions the length of the metal panel was increased to 1 m, 2 m, and 4 m while the width was constant. The simulated S_{11} of the antenna with different reflector panels length is depicted in Fig. 6. From Fig. 6 it can be observed that by implementing the reflector the bandwidth of the antenna decreases. For 50 cm, 1 m, 2 m, and 4 m of panel length, the antenna has a −10 dB bandwidth of 40.5 MHz, 42.3 MHz, 40 MHz, and 110 MHz respectively. As seen from the S_{11} plot, the panels of length less than 4 m exhibit very similar S_{11} characteristics. The reason for this is further explored by investigating the far-field radiation pattern in the coming paragraphs.

The parabolic reflector gain improvement is clearly seen in Fig. 7 which shows the gain comparison of the Vivaldi antenna with and without the reflector panels. Fig. 7 shows that by deploying the reflector metal panel the gain of
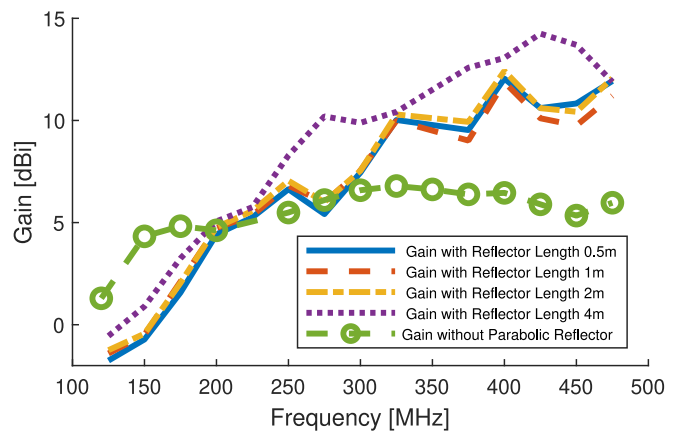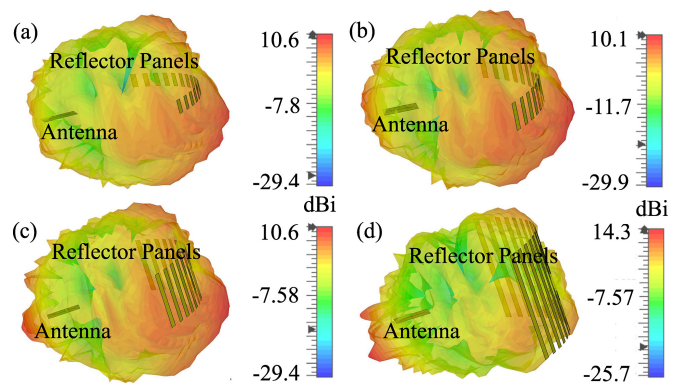
the antenna increases for most of the operating bandwidth. Below 200 MHz the gain of the antenna without the reflector panel is high, whereas, above 200 MHz the gain of the antenna with the reflector increases significantly. For the reflector panel of 50 cm, 1 m, and 2 m the gain does not vary notably and they have a maximum gain of 12.04 dBi, 11.87 dBi, and 12.42 dBi respectively occurs at 400 MHz. On the other hand, for the panel length of 4 m there is a notable increase of gain is evident. The maximum gain for 4 m panel is 14.25 dBi occurs at 425 MHz.

The far-field radiation pattern for each of the reflector panels at 425 MHz is shown in Fig. 8. Fig. 8 shows that the panels with lengths of 50 cm, 1 m, and 2 m are not working as a reflector, from the location of maximum (red) pattern we can see the peak radiation pattern has not been reflected by the panels. This also explains why the gain in Fig. 6 is very similar for panels of lengths 0.5, 1, and 2 m. For these panels, the peak radiation pattern is in the direction of maximum gain of the feed Vivaldi antenna. For these dimensions, the panels act more like director elements which incidentally provide some gain enchantment. However, the panels with a length of 4 m work as both a reflector and as well as gain enhancer. Thus, although the gain is increasing
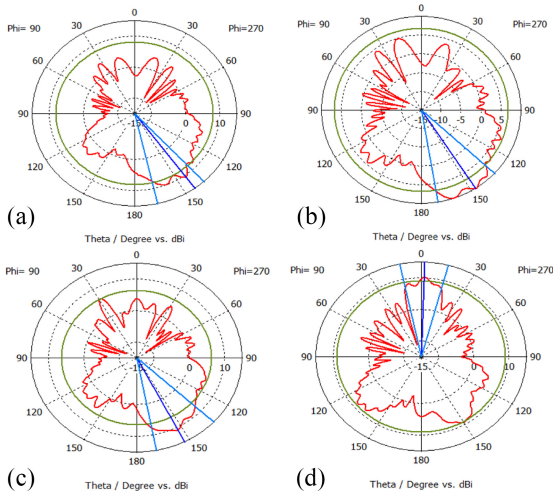
FIGURE 9. E-plane radiation pattern at $\phi = 90°$ for each of the reflector panels at 425 MHz (a) 50 cm panels (b) 1m panels (c) 2 m panels (d) 4 m panels.

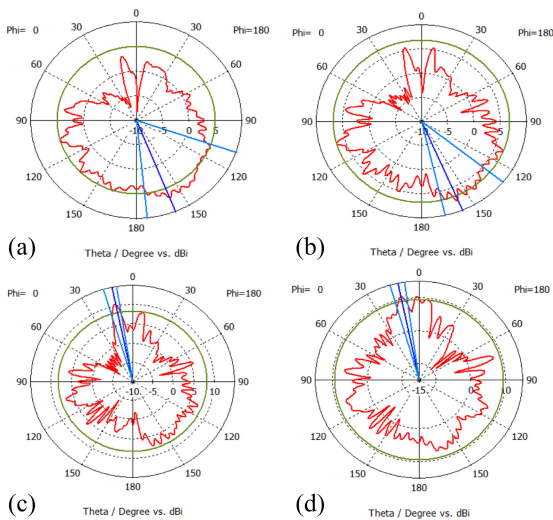**FIGURE 10.** H-plane radiation pattern at $\phi = 0°$ for each of the reflector panels at 425 MHz (a) 50 cm panels (b) 1m panels (c) 2 m panels (d) 4 m panels.

for each panel length in Fig. 7, the direction of the gain is not the same.

The phenomenon observed in Figs. 7 and 8 is because the gain and directivity of a reflector antenna is directly proportional to its aperture efficiency and this aperture efficiency is a combination of aperture taper efficiency and spillover efficiency. When the dimension of the panels is smaller, the aperture taper efficiency and spillover efficiency is low, as a consequence the panels with smaller dimension is not acting like a reflector antenna. However, with a larger panel dimension, the efficiency is high and as a result, the proposed antenna works as a reflector antenna. Figs. 9 and 10 depict the radiation pattern in the E-plane and H-plane, respectively, for each of the reflector panels operating at a frequency of 425 MHz. For a panel length of 50 cm, the E-plane radiation pattern exhibits a main lobe direction at 144° with a 3 dB beamwidth of 29.6°. For 1 m and 2 m, the main lobe

TABLE 3. Comparison between the proposed antenna with other related works.

Ref No.	Type of Antenna	Bandwidth	Gain	Operational Frequency	Air-Borne
[21]	Bow-tie antenna	4.1 GHz	7 dB	0.4 - 4.8 GHz	No
[22]	Wheel-shaped patch antenna	16.87 GHz	6 dB	3.01 - 19.88 GHz	No
[23]	Bow-tie antenna	1.85 GHz	4 dB	0.45 - 2.3 GHz	No
[24]	Umbrella-shaped patch antenna	10 GHz	3.5 dBi	2 - 14 GHz	No
[25]	Horn antenna	2.9 GHz	15.48 dB	2.6 - 4.9 GHz	No
[7]	Antipodal Vivaldi antenna	1.7 GHz	11.5 dBi	0.3 - 2 GHz	Yes
[9]	Vivaldi antenna	600 - 30000 MHz	12 dBi	500 - 3000 MHz	Yes
[Proposed Antenna]	Reflector-based Vivaldi antenna	387 MHz	14.25 dBi	100 - 500 MHz	Yes

direction shifts to 147°, and 153°, while the 3 dB beamwidth expands to 37.7°, and 36.3°, respectively. However, for 4m of panel length, the main lobe direction exhibits at 2° with a 3 dB beamwidth of 26.8°.

Moreover, we can also assert that as our antenna is operating well within the frequency band from 200 MHz to 500 MHz, the proposed antenna is able to obtain a maximum penetration depth of 2 m [19]. This proposed antenna will also have a high resolution as the resolution of the GPR antenna is directly proportional to its bandwidth [20].

A comprehensive comparative analysis has been done to compare the performance of the proposed GPR antenna with the pre-existing GPR antennas, presented in Table 3. The performance of the proposed antenna exhibits promising results when compared to the reported performances of antennas in the existing literature. Although the proposed antenna has a lower bandwidth compared to the other related works. However, the gain of the proposed antenna is comparatively high than those of pre-existing GPR antennas. Moreover, compared with other air-borne GPR antennas, the proposed antenna also exhibits a higher gain.

IV. CONCLUSION AND FUTURE WORKS

In this work, a reflector based airborne GPR antenna is proposed. The antenna has a high gain and possesses a high penetration depth of 2 m. A discrete parabolic reflector was proposed and a wideband, lightweight Vivaldi antenna was designed as a feeding structure. The operational frequency of the proposed antenna is 100–500 MHz and the antenna has a bandwidth of 387 MHz. The discrete parabolic reflector with a dimension of 30 cm by 4 m works as a reflector antenna with a maximum gain of 14.25 dBi. Our proposed antenna will also have a better resolution in the lower frequency

band due to its wideband characteristics. In future works, the antenna panel configuration will be further optimized for integration into a multi-rotor UAV system. Moreover, the maximum flight time of the UAV with payload and its' control system to maintain the desired spacing between the reflectors will also be investigated in the future. Additionally, the whole prototype will be fabricated in the future to further validated our proposed work.

REFERENCES

[1] D. Edemsky, A. Popov, I. Prokopovich, and V. Garbatsevic, "Airborne ground penetrating radar, field test," *Remote Sens.*, vol. 13, no. 4, p. 667, Feb. 2021, doi: 10.3390/rs13040667.

[2] T. Sigurdsson and T. Overgaard, "Application of GPR for 3-D visualization of geological and structural variation in a limestone formation," *J. Appl. Geophys.*, vol. 40, nos. 1–3 pp. 29–36, Oct. 1998, doi: 10.1016/S0926-9851(98)00015-9.

[3] L. B. Conyers and J. Leckebusch, "Geophysical archaeology research agendas for the future: Some ground-penetrating radar examples," *Archaeol. Prospect*, vol. 17, pp. 117–123, May 2010, doi: 10.1002/arp.379.

[4] L. Pajewski et al., "Applications of ground penetrating radar in civil engineering–COST action TU1208," in *Proc. 7th Int. Workshop Adv. Ground Penetrat. Radar* Nantes, France, 2013, pp. 1–6, doi: 10.1109/IWAGPR.2013.6601528.

[5] D. Eisenburger, H. Lentz, and M. Jenett, "Helicopter-borne GPR systems: A way from ice thickness measurements to geological applications," in *Proc. IEEE Int. Conf. Ultra-Wideband*, Hannover, Germany, 2008, pp. 161–165, doi: 10.1109/ICUWB.2008.4653441.

[6] C. Warren and A. Giannopoulos, "Investigation of the directivity of a commercial ground-penetrating radar antenna using a finite-difference time-domain antenna model," in *Proc. 14th Int. Conf. Ground Penetrat. Radar (GPR)*, Shanghai, China, Jun. 2012, pp. 226–231, doi: 10.1109/ICGPR.2012.6254865.

[7] J. Guo, J. Tong, Q. Zhao, J. Jiao, J. Huo, and C. Ma, "An ultrawide band antipodal vivaldi antenna for airborne GPR application," *IEEE Geosci. Remote Sens. Lett.*, vol. 16, no. 10, pp. 1560–1564, Oct. 2019, doi: 10.1109/LGRS.2019.2905013.

[8] J.-B. Yan, S. Gogineni, B. Camps-Raga, and J. Brozena, "A dual-polarized 2–18-GHz vivaldi array for airborne radar measurements of snow," *IEEE Trans. Antennas Propag.*, vol. 64, no. 2, pp. 781–785, Feb. 2016, doi: 10.1109/TAP.2015.2506734.

[9] M. G. Fernandez, G. A. Narciandi, A. Arboleya, C. V. Antuna, F. L.-H. Andres, and Y. A. Lopez, "Development of an airborne-based GPR system for landmine and IED detection: Antenna analysis and intercomparison," *IEEE Access.*, vol. 9, pp. 127382–127396, 2021, doi: 10.1109/ACCESS.2021.3112058.

[10] Y. Rahmat-Samii and R. Haupt, "Reflector antenna developments: A perspective on the past, present and future," *IEEE Antennas Propag. Mag.*, vol. 57, no. 2, pp. 85–95, Apr. 2015, doi: 10.1109/MAP.2015.2414534.

[11] C. A. Balanis, "Reflector antennas," in *Antenna Theory: Analysis and Design*, 4th ed. Hoboken, NJ, USA: Wiley, 2016, pp. 875–920.

[12] L. Wu, S. Peng, J. Xu, and Z. Xiao, "A W-band radiometer with the offset parabolic antenna for radiometric measurements," *Int. J. Antennas Propag.*, vol. 2016, Jan. 2016, Art. no. 4705072, doi: 10.1155/2016/4705072.

[13] J. L. Volakis, "Reflector antennas," in *Antenna Engineering Handbook*, 4th ed. New York, NY, USA: McGraw-Hill, 2007, p. 15.

[14] G. R. Olhoeft, "The new ground-penetrating radar regulatory environment," in *Proc. 9th Int. Conf. Ground Penetrat. Radar (GPR)*, Shanghai, China, Jun. 2012, pp. 226–231, doi: 10.1109/ICGPR.2012.6254865.

[15] E. J. Thomas, "FCC part 15," Federal Commun. Comm., Washington, DC, USA, Jul. 2002.

[16] Y. Yang, Y. Wang, and A. E. Fathy, "Design of compact vivaldi antenna arrays for UWB see through wall applications," *Prog. Electromagn. Res.*, vol. 82, pp. 401–418, 2008, doi: 10.2528/PIER08040601.

[17] P. J. Gibson, "The vivaldi aerial," in *Proc. 9th Eur. Microw. Conf.*, Brighton, U.K., Sep. 1979, pp. 101–105, doi: 10.1109/EUMA.1979.3326815.

[18] R. A. Marino, "Broadband fixed-radius slot antenna arrangement," U.S. Patent 6 043 785 A, Mar. 28, 2000.

[19] A. Annan, "Ground penetrating radar. Workshop notes," Sens. Softw. Inc., Mississauga, ON, Canada, Rep., 2001.

[20] D. Shi, T. Aftab, G. Gidion, F. Sayed, and L. M. Reindl, "A novel electrically small ground-penetrating radar patch antenna with a parasitic ring for respiration detection," *Sensors.*, vol. 21, no. 6, p. 1930, Mar. 2021, doi: 10.3390/s21061930.

[21] R. Nayak, S. Maiti. and S. K. Patra, "Design and simulation of compact UWB bow-tie antenna with reduced end-fire reflections for GPR applications," in *Proc. Int. Conf. Wireless Commun. Signal Process. Netw. (WiSPNET)*, Chennai, India, 2016, pp. 1786–1790, doi: 10.1109/WiSPNET.2016.7566447.

[22] P. Prasad, S. Singh, and A. Kumar, "A wheel shaped compact UWB antenna for GPR applications," in *Proc. 6th Int. Conf. Conver. Technol. (I2CT)*, Maharashtra, India, 2021, pp. 1–5, doi: 10.1109/I2CT51068.2021.9418128.

[23] H. S. Senapati, P. Chongder, K. K. Ajith, and S. Maiti, "Design Of UWB bow tie antenna For GPR object detection," in *Proc. Adv. Commun. Technol. Signal Process. (ACTS)*, Rourkela, India, 2021, pp. 1–4, doi: 10.1109/ACTS53447.2021.9708073.

[24] S. Kundu and S. K. Jana, "A compact umbrella shaped UWB antenna for ground-coupling GPR applications," *Microw. Opt. Technol. Lett.*, vol. 60, no. 1, pp. 146–151, Jan. 2018, doi: 10.1002/mop.30928.

[25] C. Ozdemir, B. Yilmaz, S. I. Keceli, H. Lezki, and O. Sutcuoglu, "Ultra wide band horn antenna design for ground penetrating radar: A feeder practice," in *Proc. 15th Int. Radar Symp. (IRS)*, Gdansk, Poland, 2014, pp. 1–4, doi: 10.1109/IRS.2014.6869298.

ZAYED MOHAMMAD (Member, IEEE) received the B.S. degree in electrical and electronic engineering from the Bangladesh University of Business and Technology, Bangladesh, in 2019. He is currently pursuing the M.S. degree in electrical and computer engineering with Idaho State University, Pocatello, ID, USA, where he is also working as a Graduate Research Assistant. He has worked as a Faculty Member with the Bangladesh University of Business and Technology.

ANDREW M. CHRYSLER (Member, IEEE) received the B.S. degree in chemical and biological engineering (with a minor in mathematics) from Colorado State University, Fort Collins, CO, USA, in 2011, and the M.S. and Ph.D. degrees in electrical and computer engineering from the University of Utah, Salt Lake City, UT, USA, in 2017 and 2018, respectively.

He is an Assistant Professor with Idaho State University. He has worked with IM Flash Technologies, Lehi, UT, USA, as a Semiconductor Manufacturing Engineer and a Co-Op with the NASA Glenn Research Center, Cleveland, OH, USA. He has also conducted research with Daegu University, Daegu, South Korea. His research interests include dielectric properties of materials, implantable antennas, millimeter-wave antennas, and international engineering education. He was an NSF EAPSI Korea Fellow in 2015 and received the IEEE APS Doctoral Research Award in 2013. He was a Center for Advanced Energy Studies Summer Faculty in 2021. He was an Air Force Research Laboratory Summer Visiting Faculty Fellow in 2022.